A FAST AND SELF-CONSISTENT APPROACH FOR MULTI-CYCLE EQUILIBRIUM CORE STUDIES USING MONTE CARLO MODELS

Zeyun Wu[1, 2]* and Robert E. Williams[1]

[1]NIST Center for Neutron Research
100 Bureau Drive, Mail Stop 6101, Gaithersburg, MD 20899 USA

[2]Department of Materials Science and Engineering
University of Maryland
College Park, MD 20742 USA
*Corresponding author: zeyun.wu@nist.gov

ABSTRACT

A fast and self-consistent approach, PRELIM approach, is described with the aim of quickly delivering a multi-cycle equilibrium core configuration using Monte Carlo models. This approach is based on simple reactor physics, and is easily incorporated into standard Monte Carlo based core simulation tools. The primary purpose of this study is to provide an efficient approach to enable routine calculations for feasibility studies of nuclear reactor design concepts based on Monte Carlo methods. The approach is capable of realistic conceptual core design calculations in a repeated manner with sufficient accuracy of key performance parameters. The validity of the PRELIM approach is demonstrated by benchmarking its results to solutions provided by a higher order approach with detailed core calculations in a given example problem.

Key Words: Multi-cycle Equilibrium Core, Reactor Physics, Monte Carlo Model

1. INTRODUCTION

The Monte Carlo (MC) method is capable of predicting the overall behavior of a nuclear reactor by individually tracing travel paths of hundreds of millions of particles created in the reactor. MC models, in many applications, are advantageous over most deterministic models in terms of flexibility in geometry allowance, detailed physics, and quantification of uncertainty. Computational models based on MC transport methodology are widely utilized in nuclear reactor design and analysis. However, the MC approach is notoriously considered as a computational costly tool because it usually relies on a very large number of random walks in order to reduce statistical uncertainty of the result to an acceptable level. For nuclear reactor analysts, the concern caused by such time-consuming burden usually prohibits the MC method from daily routine design activities, particularly in activities such as feasibility studies on a multi-cycle equilibrium core, optimization studies, parametric studies, etc. In general, the MC approach can become inefficient for tasks requiring large number of forward transport calculations.

Multi-cycle equilibrium core development, which is the very first task for a reactor physicist in reactor analysis, is one of the time-consuming tasks confronted by the MC method because most of the currently widely accepted MC codes, such as MCNP [1], are developed only for stationary

(i.e. steady state) calculations and a large number of iterations are normally required to reach an equilibrium status. Although some MC codes are extended with fuel burnup capability by combining a MC forward solver with some existing fuel depletion modules [2-5], they are more or less aimed at specific research purposes and are usually too onerous to be applied for routine jobs in reactor design. In the latest MCNP code [6], the fuel burnup feature from MCNPX [7] is incorporated as the BURN option in MCNP6, which can trace density changes of hundreds of isotopes in the reactor after specifying depletion intervals. However, experience has shown that it requires a large amount of computational resources and time when applying this feature to generate an equilibrium core [8]. In the preliminary reactor design phase, there are often many geometry and material variations to analyze and detailed fuel inventories are not needed to estimate the reactivity or the power and flux distribution.

In this paper, we present an efficient and self-consistent approach to significantly reduce the computational overhead on the MC method when applied to feasibility studies in multi-cycle reactor core design and analysis. This method is developed based on simple reactor physics and is easily implemented with minor programming efforts. Nevertheless, it can produce numerical results with an accuracy at the same level as higher order calculations. The primary goal of this work is to provide a simplified but rigorous shortcut to quickly generate an equilibrium core configuration for reactor design using MC models. It is not intended for safety analysis in which one must set some limits on power density or heat flux, but rather aimed for providing an easily-applied and self-consistent approach for feasibility studies on new reactor core designs while utilizing existing MC functions.

Given some basic core design parameters such as reactor power, fuel cycle length, initial fuel loading and desired fuel management schemes, one can roughly estimate fuel inventories at the anticipated end of cycle (EOC). Note that control elements can be generally omitted at EOC, which makes material configuration at EOC appear simpler. Thus the approach discussed here starts with an initial estimate of the fuel material for an equilibrium core at EOC using an approximate concentration of major fission product poisons. The initial values of the core inventories are then adjusted in subsequent iterations by using reaction rates of interest and thermal fluxes calculated by MC simulation so that the resulting core inventories will be self-consistent with the core performance. The iterations are continued until the core performance reaches equilibrium status. At the end, fuel contents in startup (SU) and beginning of cycle (BOC) cores can also be estimated by using the results in EOC core, fuel cycle length and core configuration.

To demonstrate the validity and efficiency of the proposed approach (denoted as PRELIM approach hereafter), MCNP6 is chosen as a typical MC based core design utility, and a research reactor, which is similar to Australia's Open Pool Australian Light-water (OPAL) reactor [9-11], is chosen as a sample problem and modeled in MCNP6. Two different approaches were applied to the problem to achieve a four-cycle equilibrium core performance with identical geometry and fuel. The first approach invoked the BURN option (henceforth denoted as BURN approach) in MCNP6 and performed very detailed depletion calculations of the core [8]. The equilibrium core configuration can be successfully achieved after tens of iterative calculations, which are obviously tedious and require very lengthy computations. Here the BURN approach works in a role of higher order calculation to provide a benchmark for the results obtained from the PRELIM approach. To initiate the calculation in MCNP, the PRELIM approach is quickly implemented in a MATLAB[a]

---

[a] Disclaimer: The identification of any commercial product or trade name in this paper does not imply endorsement or recommendation by the National Institute of Standards and Technology.

program to automatically generate proper inputs for MCNP6 such that the approach can be efficiently incorporated into MCNP6 to produce equilibrium core configuration. Comparisons of the core performance yielded from both approaches on the sample problem will be presented and discussed in the numerical example section of the paper.

The paper is organized as follows: Section 2 describes the basics underlying the PRELIM approach and the assumptions and approximations used in the approach. A detailed description of the implementation of the PRELIM approach is also presented in this section. The sample problem results are discussed in Section 3 as a proof of principle to the proposed approach. Concluding remarks and advisory comments on the approach are provided in the summary section.

2. METHOD DESCRIPTION

In the PRELIM approach, isotopes of interest in the fuel material are selected based on simple reactor physics. In a uranium fueled core, for example, the overwhelming fissionable isotopes such as U-235, U-238, Pu-239 are explicitly treated as well as the most significant fission product poisons such as Xe-135 and Sm-149. In addition, general fission product poisons (presumed with 50 barns per fission) are represented by B-10, and an optional "filler" material, Bi-209, is artificially imposed into the fuel to account for the rest of burned fuel mass. For cores with different fuel type, similar selections can be applied. The goal of the approach is to generate fuel inventories of these selected materials for equilibrium cores at SU, BOC, and EOC respectively. The resulting model can be used to perform conventional reactor physics calculations to obtain important core performance parameters such as k_{eff}, flux and power distribution, etc. Therefore, the main efforts of the PRELIM approach are spent to develop an efficient way to estimate atom densities of these selected materials. For simplicity, a uranium fueled core was picked as a representative in this section to facilitate the description of our approach.

Some fundamental knowledge on key fuel composition changes in the core are provided in Appendix A, which worked as a theoretical essence for the PRELIM approach. Based on the analysis in Appendix A, the PRELIM approach develops an equilibrium core using MC models with the following steps:

Step I: Initial Values of EOC Model

As aforementioned, the EOC model is considered first in the PRELIM approach. Since an iterative strategy is applied in the approach, the first step is to find initial values of fuel contents at EOC for an equilibrium core. The initial solution must be consistent with the expected fresh fuel loading and basic core design information such as fuel cycle length and fuel management scheme so as to provide a reasonable starting point of EOC model. Note that the initial values will be updated based on calculations of core performance (e.g., reaction rate and flux tallies) to obtain a self-consistent model in the following steps in an iterative architecture.

For a given fresh uranium fuel, the density of the fuel and U-235 enrichment are known, thus the mass fraction for each isotopic composition in the fuel can be calculated. Given the fuel material, cycle length, and power rate of the reactor, one can roughly estimate the mass of fissile material U-235 consumed per fuel element per cycle at EOC. The buildup of Pu-239 and depletion of U-238 at EOC for each fuel element can also be estimated accordingly. At this point, the accuracy of these preliminary estimates is not too important as they will be iteratively updated in the following steps.

At this step, we start to provide initial values of EOC model with an estimate of the saturated Xe-135 concentration at EOC. The solution for the equilibrium Xe-135 concentration is given by Eq.(A-6) in Appendix A. However, as the neutron flux is not known initially, Eq.(A-6) can be reduced to the form of

$$N_X^\infty = \frac{(\gamma_X + \gamma_I)\Sigma_f}{\sigma_a^X} \approx \frac{(\gamma_X^{25} + \gamma_I^{25})\sigma_f^{25} N_{25} + (\gamma_X^{49} + \gamma_I^{49})\sigma_f^{49} N_{49}}{\sigma_a^X} \tag{1}$$

by assuming the radioactive decay rate of xenon is negligible with respect to the absorption loss, i.e.,

$$\sigma_a^X \phi_0 \gg \lambda_X . \tag{2}$$

The meanings of the symbols used in the equation are provided in Appendix A, and the superscripts for heavy actinides are followed with the Los Alamos National Lab (LANL) convention, namely combining the last digits of atomic and mass number of the actinide. Note that the xenon concentration is slightly overestimated by applying this assumption, but this is a good assumption for high flux reactors.

Sm-149 can be analyzed in a similar manner, and the initial Sm-149 concentration is obtained as a form of (see Eq.(A-12))

$$N_S^\infty = \frac{\gamma_P \Sigma_f}{\sigma_a^S} \approx \frac{\gamma_P^{25} \sigma_f^{25} N_{25} + \gamma_P^{49} \sigma_f^{49} N_{49}}{\sigma_a^S} . \tag{3}$$

In the PRELIM approach, all other fission product poisons besides Xe-135 and Sm-149 are represented by boron (B-10) with the assumption that the amount of other fission product poison is proportional to the quantity of U-235 undergoing fission, that is

$$\sigma_a^B N_B = \sigma_g \left(N_{25}^0 - N_{25}\right) \frac{\sigma_f^{25}}{\sigma_a^{25}} . \tag{4}$$

Here σ_g (= 50 barn) represents the microscopic absorption cross section of a general fission product poison, and N_{25}^0 is U-235 atom density in fresh fuel.

Finally, an optional "filler" material, Bi-209, is used in the PRELIM approach to account for the rest of burned fuel mass to preserve the same fuel density as fresh fuel. This completes the first step of the approach to provide initial values of fuel contents for EOC calculations. Note that all these initial values are independent of the neutron flux; they will be modified in the following steps with calculated fission rates and thermal fluxes to obtain self-consistent results.

Step II: Iterations on EOC Model

After the MC calculation with the initial values for EOC model, reaction rates and thermal flux for each fuel region are available. These results can be used to adjust the concentration of the fuel constituents, assuming the EOC results are "reasonable" (i.e., k_{eff} = 1.0). This is the basic idea behind the so called 'self-consistent' principle in the PRELIM approach.

To update the concentration of Sm-149, we assume the production rate of Sm-149 should be equal to its removal rate due to neutron absorption because it normally reaches equilibrium status

in a few days of reactor operation. Thus the ratio of the fission rate and Sm-149 removal rate can be used to indicate if the correct Sm-149 concentration is being obtained. If the ratio is close to unity, the estimate of Sm-149 concentration is good enough for EOC result, otherwise Sm-149 density can be updated as follows

$$N_S' = N_S \frac{\gamma_P R_f}{R_S} = N_S \frac{\gamma_P^{25} R_f^{25} + \gamma_P^{49} R_f^{49}}{R_S} \, . \tag{5}$$

Here N_S is the Sm-149 density estimated in previous iteration. R_f^{25}, R_f^{49} are fission rates of U-235 and Pu-239 respectively, and R_S is Sm-149 removal rate. These three quantities can be obtained from the calculation in the previous iteration.

The Xe-135 density is updated by using Eq.(A-6) directly without applying the assumption given by Eq.(2). Two quantities are required here: R_f = fission rate and R_X = Xe-135 removal rate. The updating scheme for Xe-135 density at this step is

$$N_X' = \frac{(\gamma_X + \gamma_I) R_f}{\lambda_X + R_X / N_X} = \frac{(\gamma_X^{25} + \gamma_I^{25}) R_f^{25} + (\gamma_X^{49} + \gamma_I^{49}) R_f^{49}}{\lambda_X + R_X / N_X} \, . \tag{6}$$

Here N_X is the Xe-135 density estimated in previous iteration.

A similar self-consistent philosophy is applied to update the B-10 concentration to represent accurate amount of minor fission product poisons, which are assumed to be proportional to the mount of U-235 undergoing fission under a given flux. Therefore the B-10 absorption rate can be described as

$$R_B' = (\sigma_g \cdot 10^{-24})(N_{25}^0 - N_{25}) \frac{\sigma_f^{25}}{\sigma_a^{25}} \varphi_{th} \tag{7}$$

Here σ_g = 50 b as being introduced before, φ_{th} is the calculated thermal flux and is presumably written in the unit of n/cm²-s. It is also noted that the atom density symbols used in all the equations are in the unit of atoms/cm³. And if the B-10 absorption rate yielded from the MC calculation is R_B, it is readily to have

$$\frac{R_B'}{R_B} = \frac{N_B'}{N_B} \, . \tag{8}$$

By combining Eq.(7) and Eq.(8), we get the updating scheme for the B-10 concentration,

$$N_B' = \frac{(\sigma_g \cdot 10^{-24})(N_{25}^0 - N_{25}) \varphi_{th}}{R_B} \frac{\sigma_f^{25}}{\sigma_a^{25}} N_B \, . \tag{9}$$

Because the total removal (including capture and fission) rate density of U-235 can be calculated in iterative steps, the exact mass of consumed U-235 for each burnt fuel element in each cycle can be estimated as follows

$$m_{25} = \frac{N_{\text{tot}}^{25}}{N_A} M_{25} = \frac{R_{25}VT_c}{N_A} M_{25}. \tag{10}$$

Here $R_{25} = R_f^{25} + R_\gamma^{25}$ is U-235 removal rate density provided by MC calculation, V is the fuel volume of the fuel element, T_c is the pre-determined fuel cycle length of the reactor, M_{25} is the atomic mass of U-235, and N_A is the Avogadro constant. The consumed mass is then used to update remaining concentration as well as the mass fraction of U-235 in the fuel at EOC. At this point, the actual accumulated Pu-239 at EOC can also be calculated based on Eq.(A-16). However, two more MC results are used to replace the flux terms in the equation. Firstly, the capture rate of U-238 can be directly calculated,

$$\sigma_\gamma^{28} N_{28}\phi_0 = R_{28}. \tag{11}$$

Secondly, the quantity $\left(\sigma_\gamma^{49} + \sigma_f^{49}\right)\phi_0$ can be estimated by the removal (including both fission and capture loss) rate of Pu-239, where we define

$$\left(\sigma_\gamma^{49} + \sigma_f^{49}\right)\phi_0 = \frac{R_{49}}{N_{49}} \equiv \lambda_{49}. \tag{12}$$

Substituting Eq.(11) and (12) into Eq.(A-16) yields the solution to estimate the Pu-239 concentration at EOC with the cycle length T_c,

$$N_{49} = N_{49}^{SU} e^{-\lambda_{49}T_c} + R_{28}\left[\frac{1-e^{-\lambda_{49}T_c}}{\lambda_{49}} + \frac{e^{-\lambda_{49}T} - e^{-\lambda_{39}T_c}}{\lambda_{49} - \lambda_{39}}\right]. \tag{13}$$

Note here the treatment to calculate Pu-239 concentration at EOC is a little bit different from the one used for Xe-135 and Sm-149. We have to use Eq.(13) to calculate the Pu-239 concentration at EOC because normally λ_{49} is not large enough to make Pu-239 to reach equilibrium with one cycle length (which is typically about 30 days for research reactors). Once the mass fraction of Pu-239 is calculated, the mass fraction of U-238 can be reduced accordingly. Finally, the mass fraction of filler material, Bi-209, can also be updated.

The iterations described above continue until the core performance reaches equilibrium status. The example discussed in Section 3 for a LEU fueled research reactor analysis shows that it usually only takes two or three iterations to achieve equilibrium core behavior.

Step III: Startup (SU) Core Model

If the k_{eff} obtained at EOC is reasonable, these results can be used to develop startup (SU) model. The SU core is assumed to have partially inserted control elements. For a standard research reactor, as an example, there is 8% - 10% excess reactivity in addition to at least a 15% shutdown margin. For the SU core, there is no Xe in any fuel, and there is no Sm, Pu, B nor Bi in fresh fuel. If the period between cycles is a week or so, we can assume Pm-149 (decay half-life is 2.2 days) has all converted to Sm-149, and Np-239 (decay half-life is 2.4 days) has all converted to Pu-239.

To obtain an accurate Sm-149 concentration at SU, we first use Eq.(A-11) to calculate equilibrium concentration of Pm-149

$$N_P^\infty = N_P^{EOC} = \frac{\gamma_P \Sigma_f \phi_0}{\lambda_P} = \frac{\gamma_P R_f}{\lambda_P} = \frac{\gamma_P^{25} R_f^{25} + \gamma_P^{49} R_f^{49}}{\lambda_P}, \tag{14}$$

and then add it to the equilibrium Sm-149 EOC concentration to produce the Sm-149 SU concentration, that is

$$N_S^{SU} = N_S^{EOC} + N_P^{EOC}. \tag{15}$$

Similarly, the equilibrium EOC concentration of Np-239 must be added to obtain Pu-239 SU concentration. The equilibrium concentration of Np-239 is (see Eq.(A-15))

$$N_{39}^\infty = N_{39}^{EOC} = \frac{\sigma_\gamma^{28} N_{28} \phi_0}{\lambda_{39}} = \frac{R_{28}}{\lambda_{39}}. \tag{16}$$

Thus the Pu-239 SU concentration for the next burnt cycle is

$$N_{49}^{SU} = N_{49}^{EOC} + N_{39}^{EOC}. \tag{17}$$

The concentration of all other material constituents such U-235, U-238, B-10, etc. at SU can be assumed to be unchanged to the one in EOC model in the previous burnt cycle. Finally the concentration of Bi-209 needs to be adjusted in order to preserve the fuel density.

Step IV: BOC Core Model

The BOC core here is defined as the SU core with addition of equilibrium concentration of Xe-135 in the fuel. Physically, xenon reaches saturation status about one day into the cycle. Therefore the mass concentration of Xe-135 at EOC can be used as Xe-135 concentration for BOC model with the assumption of uniform fission density throughout. Strictly, Eq.(A-10) and Eq.(A-16) must be used to calculate Sm-149 and Pu-239 concentration at BOC with the known of time period from SU to BOC (usually it takes $1 - 2$ days), that is

$$N_S^{BOC} = S^{SU} e^{-\lambda_S T_B} + \gamma_P R_f \left[\frac{1 - e^{-\lambda_S T_B}}{\lambda_S} + \frac{e^{-\lambda_S T_B} - e^{-\lambda_P T_B}}{\lambda_S - \lambda_P} \right]$$

$$N_{49}^{BOC} = N_{49}^{SU} e^{-\lambda_{49} T_B} + R_{28} \left[\frac{1 - e^{-\lambda_{49} T_B}}{\lambda_{49}} + \frac{e^{-\lambda_{49} T_B} - e^{-\lambda_{39} T_B}}{\lambda_{49} - \lambda_{39}} \right]$$

where $\lambda_S = \sigma_a^S \phi_0 = R_S / N_S$, $\lambda_{49} = R_{49} / N_{49}$, and T_B is the time length needed from SU to BOC. For simplicity, as in the implementation of the PRELIM approach, the Sm and Pu concentrations at BOC are obtained as the average of the SU and EOC values for a specific fuel material.

3. NUMERICAL EXAMPLE

A generic version of a 20 MW$_{th}$ beam tube research reactor, which is similar to Australia's OPAL reactor [9-11], was modeled here as a demonstrative example to validate the accuracy and the efficiency of PRELIM approach. OPAL is a research reactor designed principally for neutron beam science and radioisotope production. It operates at a power of 20 MW$_{th}$ in cycles of 33 days on and 2 days off year-round. Its compact core consists of 16 plate type fuel elements. The core is cooled and partly moderated by light water, while the entire core is surrounded by a heavy water

reflector in order to maximize thermal neutron flux. The core and heavy water reflector is cooled and shielded with a large open water pool.

MCNP6 is adopted to model the reactor. As the purpose here is to show the validity of the proposed approach, the numerical example developed with MCNP6 is not exactly a duplicate of the OPAL reactor but has similar geometry and fuel parameters. Some key design parameters of the model used in the example are listed in Table I.

Table I. Design Parameters of the Research Reactor Developed by MCNP6

Power (MW$_{th}$)	20
Fuel cycle length (days)	30
Days between cycles	7
Fuel cycle batches	4
Fuel element (FE) layout	4 x 4
Fuel type	MTR[1]
Number of fuel plates per FE	17
Fuel material	U_3Si_2
Fuel enrichment (%)	19.75
Fuel density (g/cc)	6.52
Fuel volume per FE (cc)	412.94

[1]MTR stands for Materials Test Reactor

The fuel enrichment and fuel density in the example are chosen to be similar to those specified in the OPAL safety analysis report [12], whereas the fuel plate size and number in the model are slightly modified to ensure the total fissile material loading in the core remains similar to that of the OPAL core. The compact core is cooled and moderated with light water, surrounded by a reflecting heavy water tank and a shielding light water pool. A schematic view of the reactor model in MCNP6 is shown in Fig. 1.

The light water channel box and heavy water container is modeled with aluminum alloy (Alloy 6061). The reactor core is fueled with 16 LEU fuel elements with nominal U-235 enrichment 19.75%. Each MTR fuel element is constructed of 17 fuel plates. The fuel is U_3Si_2 in an aluminum powder dispersion that is clad in aluminum alloy. The density of the fuel meat is 6.52 g/cc. Fig. 2 depicts the fuel element layout and water channel box frame in the center of the reactor. The batch number of each fuel element indicating the fuel management scheme applied to the problem is also shown in Fig. 2.

(a) X–Z view   **(b) X-Y view**
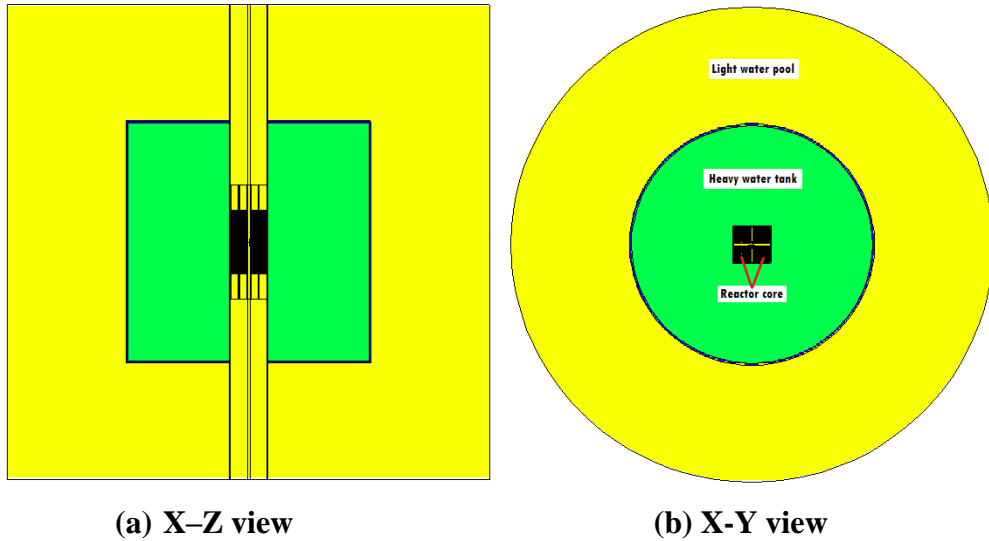
Figure 1. A schematic view of cutaway side-plane (left) and mid-plane (right) of the reactor.
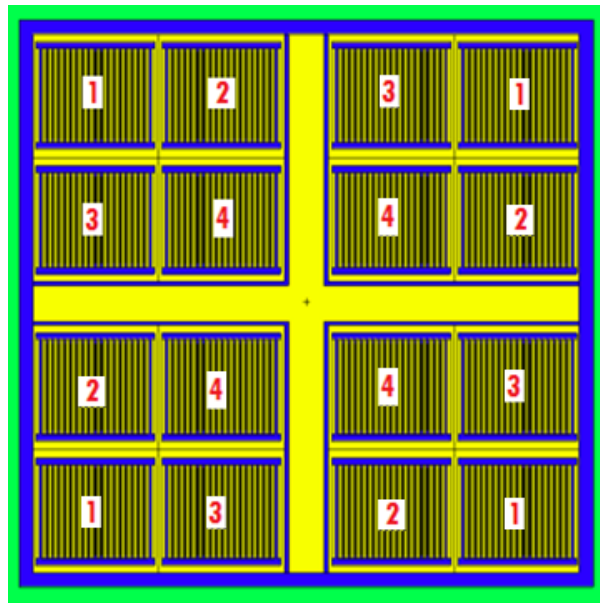
Figure 2. Fuel element layout in the core.

The core is configured in a symmetric 4 × 4 layout geometry. The cross sectional wide water gaps in the core is the space intentionally left for reactor control elements, but they are not modeled here because this paper is mainly focused on EOC. As the principal objective of our study is to quickly determine the four-cycle equilibrium core constituents for the model to carry out conventional core design calculations, we did not spend time on the fuel management scheme but rather employ a standard out-in loading strategy [13] for the fuel loading. The loading and shuffling scheme for fuel elements in the core is shown as red numbers in Figure 2, in which the number 1 stands for the fresh fuel at BOC, and number 4 stands for the discard fuel at EOC.

To obtain a multi-cycle equilibrium core configuration, two approaches were applied to the problem with identical geometry and fuel management scheme as given above. The first approach, BURN approach, employed the MCNP6 intrinsic BURN option to invoke detailed depletion calculation of the fuel material of interest. In this case, all fuel materials in the core need to be treated individually. The resulting output of the calculation is so lengthy that it is necessary to develop some auxiliary utilities to assist manipulating the large amount of output in the BURN approach. The BURN approach also relies on an iterative strategy to achieve the equilibrium core behavior. The fuel elements in the next iteration are replaced with the results yielded from the previous iteration following the pre-specified fuel loading and shuffling scheme. The process can start with a reasonable estimation of the fuel contents or simply with all fresh fuel elements (the latter option is the one used in the work). The iterations are stopped when the core reaches equilibrium status, in which the key performance parameters of the core remain statistically constant. A detailed description of the BURN approach on equilibrium core generation can be found in Ref. [8].

The second approach, PRELIM approach, implements the methodology described in Section 2 into a MATLAB based program, which can generate MCNP6 inputs with the given core design parameters presented in Table I. The program first produces an initial estimate of the fuel contents in each fuel element at EOC and then calls MCNP6 to perform core calculations. After the calculation completes, the program can read in the required tally information from the MCNP output file and create fuel contents in MCNP format for the next iteration. The iteration is stopped when the fraction of fuel material composition remains statistically unchanged. The convergence usually occurs within 3 or 4 iterations.
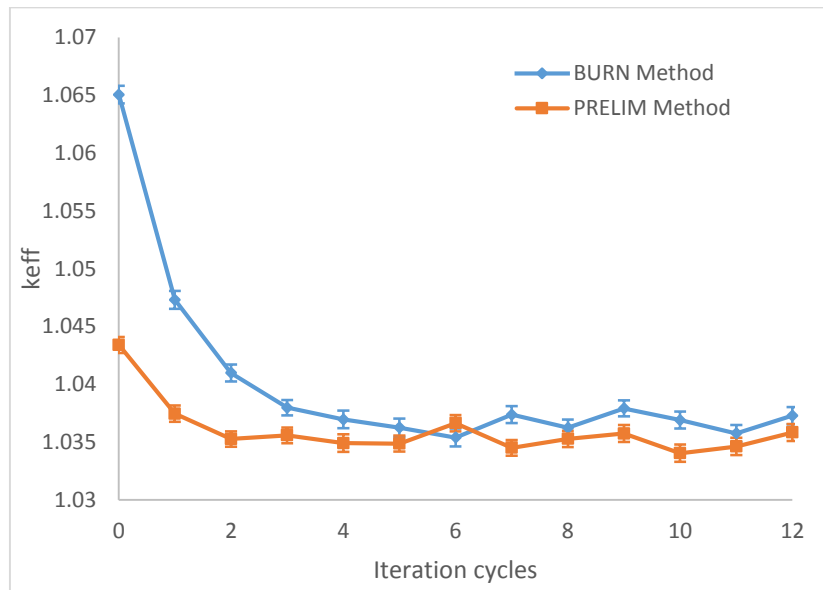
Figure 3. Comparison of EOC k_{eff} changes with iterative cycles in both approaches.

The k_{eff} at EOC as a function of iteration number for the example problem is shown in Fig. 3. Two line plots with 1-σ statistical error bar (i.e., 68% confidence level) represent the k_{eff} trends of the BURN and the PRELIM approaches, respectively. For time saving purpose, all the criticality

calculations carried out in MCNP are using 5000 particles per cycle for 210 cycles with 10 inactive cycles skipped, in which the statistical errors of k-eigenvalue are within 50 pcm (per cent mille).

As shown in the figure, the k_{eff} yielded from the two approaches have significant difference in the first few iterations, this is mainly because the BURN approach used all fresh fuel at the starting point. After about 4 iterations, the two k_{eff} curves both asymptotically converge to roughly the same value at EOC. Note that if considering 3-σ statistical error bar (i.e. in 99% confidence level), both approaches can be considered to be ended up with identical result in k_{eff}.

As far as the computation time concerned, the BURN approach embedded in MCNP6 employs the predictor-corrector method to perform burnup calculations, which implies the flux calculation (the most time consuming step) is performed twice at every burnup step in the approach. And to obtain reasonably accurate results at EOC, several burnup steps are usually required in the BURN approach for one cycle calculation. Due to these reasons, the computational time demanded by the BURN approach is far more than the time needed in the PRELIM approach. In the example problem, with the same number of starting particles provided for the *kcode* calculation in MCNP (200 active cycles with 5000 particles per cycle), the average computation time is about 200 minutes per iteration cycle in the BURN approach, while the proposed PRELIM approach only takes about 6 minutes to complete one iteration cycle calculation. Note the time compared here is the wall clock time on executing MCNP6 in a single desktop with 8 processor CPUs at 3.40 GHz. Moreover, the human intervention time spent in the PRELIM approach is nearly negligible once the methodology is implemented and the updated fuel inventories are produced automatically. As a matter of fact, more human time is spent in the BURN approach for data processing because the BURN approach tracks over 200 hundred isotopes explicitly in the burnup calculation and generates very lengthy output file.

Table II summarizes the k_{eff} at startup (SU) and beginning of cycle (BOC) stage estimated from both approaches using the EOC results after 12 iterations. Somewhat bigger deviations between the two approaches are identified for SU and BOC. However, these results are still acceptable with the consideration of the magnitude of statistical errors introduced by MCNP for the results (see Table II).

Table II. k_{eff} at SU, BOC, and EOC in both approaches.

Stage	BURN	PRELIM	Deviation
SU	1.11535 $\pm$ 0.00084	1.11442 $\pm$ 0.00090	0.00093
BOC	1.07756 $\pm$ 0.00075	1.07521 $\pm$ 0.00083	0.00235
EOC	1.03729 $\pm$ 0.00083	1.03583 $\pm$ 0.00076	0.00146

To make a further assessment of the PRELIM approach, the mass fractions of some key isotopes in burnt fuel at EOC predicted by both approaches are compared in Table III. It appears the PRELIM approach predicts burnup of major fissile material U-235 and production of Xe-135 fairly well (less than ~3% difference from BURN approach). However, the prediction of the buildup of Pu-239 and the production of Sm-149 have unacceptable large deviations compared to results from higher order calculation. However, they are relatively minor constituents and the associated uncertainties are also high, thus these less reliable values have less impact of the resulting core performance.

Table III. Prediction of mass fractions of some key isotopes in burnt fuels at EOC

		U-235	Pu-239	Xe-135	Sm-149
Once burnt fuel	**BURN**	1.27E-01	1.09E-03	8.63E-07	6.95E-06
	PRELIM	1.27E-01	1.19E-03	8.78E-07	7.31E-06
	Difference (%)	**-0.61**	**8.51**	**1.78**	**5.17**
Twice burnt fuel	**BURN**	1.10E-01	2.05E-03	7.66E-07	6.46E-06
	PRELIM	1.08E-01	2.19E-03	7.81E-07	6.54E-06
	Difference (%)	**-1.58**	**7.10**	**1.86**	**1.22**
Third burnt fuel	**BURN**	9.40E-02	2.74E-03	6.69E-07	5.94E-06
	PRELIM	9.14E-02	2.87E-03	6.72E-07	5.70E-06
	Difference (%)	**-2.7494**	**4.75**	**0.46**	**-4.06**
Fourth burnt fuel	**BURN**	7.85E-02	3.19E-03	5.75E-07	5.36E-06
	PRELIM	7.58E-02	3.27E-03	5.62E-07	4.81E-06
	Difference (%)	**-3.39**	**2.63**	**-2.32**	**-10.34**
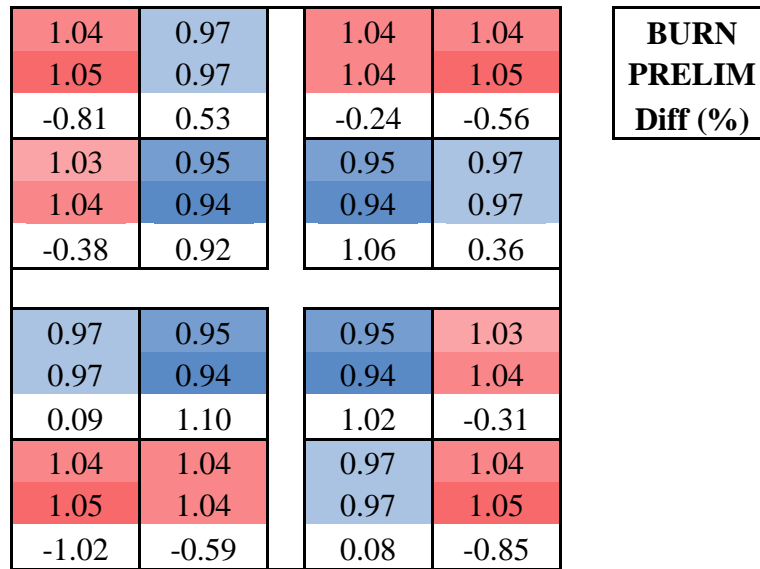
Figure 4. The power factors of fuel elements predicted by the two approaches. A group of three values are shown for each fuel element: The first value is the power factor predicted by the BURN approach, the second value is the one predicted by the PRELIM approach, and the last one gives the relative difference between these two. Colors in the figure indicates the magnitude of the normalized power of the FE.

The power distribution of the core is also important for the reactor analyst to perform feasibility studies and safety analyses. Detailed 3-D power density calculation for the sample problem was performed using the fuel material inventories yielded from both BURN and PRELIM approaches. The total peaking power factor for the model core obtained from BURN and PRELIM

approaches are 2.1405 and 2.1388, respectively. The power factor distribution among the fuel elements obtained from the two approaches are shown in Figure 4, in which the fuels with power slightly higher than the average are shown with red background, the others are blue. As can be seen, the differences existing in the fuel element-wise power factors from two approaches are either less than or very close to 1%. All these results simply indicate the PRELIM approach is able to predict the power of the core as accurately as the one from the higher order approach.

4. SUMMARY

A fast and self-consistent approach, PRELIM approach, is presented to quickly achieve multi-cycle equilibrium core for feasibility studies in new reactor design using MC models. The approach is based on simple reactor physics, and is easy to incorporate with standard MC core design tools. The computational time required to produce an equilibrium core, as shown in the example, is significantly reduced comparing to the approach introduced by the latest MCNP code. The primary advantage of this proposed approach is that it enables conceptual core design calculations in a repeated manner with sufficient accuracy on key design performance parameters such as k_{eff}, flux and power distribution, etc. The approach is desirable in core feasibility studies but once a conceptual design is chosen, more rigorous methods are needed for fuel depletion analyses and the reactor safety analysis.

5. REFERENCES

1. "MCNP – A General Monte Carlo N-Particle Transport Code, Version 5," LA-UR-03-1987, Los Alamos National Laboratory, April 24 (2003).

2. R. L. Moore, B. G. Schnitzler, C. A. Wemple, R. S. Babcock, And D. E. Wessol, "MOCUP: MCNP-ORIGEN2 Coupled Utility Program," INEL-95/0523, Idaho National Engineering Laboratory (1995).

3. D. I. Poston and H. R. Trellue, "User's Manual Version 2.0 for MONTEBURNS, Version 5B," LA-UR-99-4999, Los Alamos National Laboratory (1999).

4. W. Haeck and B. Verboomen, "An Optimum Approach to Monte Carlo Burn-Up," Nuclear Science and Engineering, **156**, p. 180-196 (2007).

5. Z. Xu and P. Hejzlar, "MCODE, Version 2.2: An MCNPORIGEN Depletion Program," MIT-NFC-TR-104, Massachusetts Institute of Technology (2008).

6. D.B. Pelowitz, Ed., "MCNP6TM User's Manual," LA-CP-11-01708, Los Alamos National Laboratory, December (2012).

7. D.B. Pelowitz, Ed., "MCNPX User's Manual version 2.6.0," LA-CP-07-1473, Los Alamos National Laboratory, April (2008).

8. A. Hanson and D. Diamond, "A Neutronics Methodology for the NIST Research Reactor Based on MCNPX," in the 19th International Conference on Nuclear Engineering (ICONE-19), Chiba, Japan, May 16-19 (2011).

9. R. Miller and P. M. Abbate, "Australia's New High Performance Research Reactor," in the 9th Meeting of the International Group on Research Reactors (IGORR-9), Sydney, Australia, March 24-28 (2003)

10. S. J. Kennedy, "Construction of the Neutron Beam Facility at Australia's OPAL Research Reactor," PHYSICA B **385-386**, p.949-954 (2006)

11. S. Kim, "The OPAL (Open Pool Australian Light-water) Reactor in Australia", Nuclear Engineering and Technology, **39**(5), p. 443-448, Special issue on HANARO, (2005)

12. OPAL Reactor SAR, http://www.arpansa.gov.au/Regulation/opal/op_applic.cfm

13. J. J. Duderstadt and L. J. Hamilton, Nuclear Reactor Analysis, John Wiley & Sons, (1976)

APPENDIX A

In a standard isotopic decay scheme, Xe-135 can be produced by three paths: one from direct fission product yield, one from beta decay of I-135, which is a product of beta decay of Te-135, and one from gamma decay of isometric Xe-135m. The decay of Te-135 to I-135 can be assumed to be instantaneous, and the short-lived isomeric state Xe-135m can be ignored by assuming all I-135 nuclei will decay directly to ground state Xe-135 [13]. With these considerations, the variation rate for I-135 and Xe-135 atomic densities can be described with the following coupled equations

I-135:
$$\frac{\partial N_I(t)}{\partial t} = \gamma_I \Sigma_f \phi(t) - \lambda_I N_I(t) \tag{A-1}$$

Xe-135:
$$\frac{\partial N_X(t)}{\partial t} = \gamma_X \Sigma_f \phi(t) + \lambda_I N_I(t) - \lambda_X N_X(t) - \sigma_a^X \phi(t) N_X(t) \tag{A-2}$$

Here $N_I(t)$ and $N_X(t)$ denote the atom densities of I-135 and Xe-135 respectively at time t, γ_I and γ_X denote the effective fission product yield of I-135 and Xe-135, λ_I and λ_X are the β-decay constants for these two isotopes, and the cross sections (Σ_f and σ_a^X) and neutron flux $\phi(t)$ are to be interpreted as one-group averages.

In the case of a clean core startup (without any fission product poison at the initial time), with the given initial condition $N_I(0) = N_X(0) = 0$ and steady state flux ϕ_0, the coupled equations can be solved for buildup of I-135 and Xe-135 as a function of time:

$$N_I(t) = \frac{\gamma_I \Sigma_f \phi_0}{\lambda_I} \left(1 - e^{-\lambda_I t}\right), \tag{A-3}$$

$$N_X(t) = \frac{(\gamma_X + \gamma_I)\Sigma_f \phi_0}{\lambda_X + \sigma_a^X \phi_0} \left[1 - e^{-\left(\lambda_X + \sigma_a^X \phi_0\right)t}\right] + \frac{\gamma_I \Sigma_f \phi_0}{\lambda_X - \lambda_I + \sigma_a^X \phi_0} \left[e^{-\left(\lambda_X + \sigma_a^X \phi_0\right)t} - e^{-\lambda_I t}\right]. \tag{A-4}$$

Of particular interest here are equilibrium concentrations of I-135 and Xe-135, which can be obtained by reducing the transient terms from solutions in Eq.(A-3) and (A-4) as follows

$$N_I^\infty = \frac{\gamma_I \Sigma_f \phi_0}{\lambda_I}, \tag{A-5}$$

$$N_X^\infty = \frac{(\gamma_X + \gamma_I)\Sigma_f \phi_0}{\lambda_X + \sigma_a^X \phi_0}. \tag{A-6}$$

That is, the concentration of these fission product poisons in a reactor operation at constant flux will eventually saturate at those equilibrium values for which the production of poisons from fission is just balanced by the decay and neutron capture losses of the poisons.

A very similar analysis can be applied to Sm-149, which is also characterized with a large fission yield and absorption cross section. It is consistent to neglect the short lived Nd-149 and assume fission yields Pm-149 directly. The resulting rate change equations are then

Pm-149:
$$\frac{\partial N_P(t)}{\partial t} = \gamma_P \Sigma_f \phi(t) - \lambda_P N_P(t) \tag{A-7}$$

Sm-149:
$$\frac{\partial N_S(t)}{\partial t} = \lambda_P N_P(t) - \sigma_a^S \phi(t) N_S(t) \tag{A-8}$$

With the given of steady state flux and assume $N_P(0) = 0$ and $N_S(0) = N_S^{SU}$ (note that Sm-149 is not necessary to be zero at the initial time as it is a stable isotope unlike Xe-135), the solutions of Eq.(A-7) and (A-8) are given as

$$N_P(t) = \frac{\gamma_P \Sigma_f \phi_0}{\lambda_P}\left(1 - e^{-\lambda_P t}\right), \tag{A-9}$$

$$N_S(t) = S^{SU} e^{-\sigma_a^S \phi_0 t} + \gamma_P \Sigma_f \phi_0 \left[\frac{1 - e^{-\sigma_a^S \phi_0 t}}{\sigma_a^S \phi_0} + \frac{e^{-\sigma_a^S \phi_0 t} - e^{-\lambda_P t}}{\sigma_a^S \phi_0 - \lambda_P} \right]. \tag{A-10}$$

The equilibrium concentrations can again be obtained by eliminating all the transient terms in Eq.(A-9) and (A-10)

$$N_P^\infty = \frac{\gamma_P \Sigma_f \phi_0}{\lambda_P}, \tag{A-11}$$

$$N_S^\infty = \frac{\gamma_P \Sigma_f \phi_0}{\sigma_a^S \phi_0} = \frac{\gamma_P \Sigma_{f0}}{\sigma_a^S}. \tag{A-12}$$

The depletion of U-238 is accompanied with build-up of Np-239 and Pu-239, whose change rate equations are described as follows

Np-239:
$$\frac{\partial N_{39}(t)}{\partial t} = \sigma_\gamma^{28} N_{28} \phi(t) - \lambda_{39} N_{39}(t), \tag{A-13}$$

Pu-239:
$$\frac{\partial N_{49}(t)}{\partial t} = \lambda_{39} N_{39}(t) - \left(\sigma_\gamma^{49} + \sigma_f^{49}\right)\phi(t) N_{49}(t). \tag{A-14}$$

Similar to the analysis on Sm-149 decay schemes (with the initial conditions given as $N_{39}(0) = 0$ and $N_{49}(0) = N_{49}^{SU}$), the concentration of Np-239 and Pu-239 are obtained

$$N_{39}(t) = \frac{\sigma_\gamma^{28} N_{28} \phi_0}{\lambda_{39}}\left(1 - e^{-\lambda_{39} t}\right), \tag{A-15}$$

$$N_{49}(t) = N_{49}^{SU} e^{-\left(\sigma_\gamma^{49} + \sigma_f^{49}\right)\phi_0 t} + \sigma_\gamma^{28} N_{28} \phi_0 \left[\frac{1 - e^{-\left(\sigma_\gamma^{49} + \sigma_f^{49}\right)\phi_0 t}}{\left(\sigma_\gamma^{49} + \sigma_f^{49}\right)\phi_0} + \frac{e^{-\left(\sigma_\gamma^{49} + \sigma_f^{49}\right)\phi_0 t} - e^{-\lambda_{39} t}}{\left(\sigma_\gamma^{49} + \sigma_f^{49}\right)\phi_0 - \lambda_{39}} \right]. \tag{A-16}$$